Ultrasound in Med. & Biol., Vol. 36, No. 6, pp. 1008–1021, 2010

0301-5629/$–see front matter

ELSEVIER

doi:10.1016/j.ultrasmedbio.2010.03.011

● *Original Contribution*

SAVING CELLS FROM ULTRASOUND-INDUCED APOPTOSIS: QUANTIFICATION OF CELL DEATH AND UPTAKE FOLLOWING SONICATION AND EFFECTS OF TARGETED CALCIUM CHELATION

J. D. Hutcheson, R. K. Schlicher, H. K. Hicks, and M. R. Prausnitz
School of Chemical and Biomolecular Engineering, Georgia Institute of Technology, Atlanta, GA, USA

(*Received* 4 *February* 2009; *revised* 11 *March* 2010; *in final form* 15 *March* 2010)

Abstract—Applications of ultrasound for noninvasive drug and gene delivery have been limited by associated cell death as a result of sonication. In this study, we sought to quantify the distribution of cellular bioeffects caused by low-frequency ultrasound (24 kHz) and test the hypothesis that Ca^{2+} chelation after sonication can shift this distribution by saving cells from death by apoptosis. Using flow cytometry, we quantitatively categorized sonicated cells among four populations: (i) cells that appear largely unaffected, (ii) cells reversibly permeabilized, (iii) cells rendered nonviable during sonication and (iv) cells that appear to be viable shortly after sonication, but later undergo apoptosis and die. By monitoring cells for 6 h after ultrasound exposure, we found that up to 15% of intact cells fell into this final category. Those apoptotic cells initially had the highest levels of uptake of a marker compound, calcein; also had highly elevated levels of intracellular Ca^{2+}; and contained an estimated plasma membrane wound radius of 100–300 nm. Finally, we showed that chelation of intracellular Ca^{2+} after sonication reduced apoptosis by up to 44%, thereby providing a strategy to save cells. We conclude that cells can be saved from ultrasound-induced death by appropriate selection of ultrasound conditions and Ca^{2+} chelation after sonication. (E-mail: prausnitz@gatech.edu) **© 2010 World Federation for Ultrasound in Medicine & Biology.**

Key Words: **Ultrasound, Bioeffects, Apoptosis, Calcium, Chelation, Drug delivery.**

INTRODUCTION AND BACKGROUND

With advances in medicine and pharmaceutical technologies, patient treatment options are often limited not by the availability of drug and biological therapeutics, but by the ability to deliver a drug to a desired location within the body while avoiding side effects caused by drug interaction with unintended targets (Langer 2001; Allen and Cullis 2004). Unfortunately, most current drug delivery routes lack the ability to target a particular site and rely on normal physiological processes to determine the biodistribution of drugs. This results in drugs inadvertently reaching other cells and tissues or being destroyed by bodily clearance mechanisms, often without reaching their intended targets.

The ultimate target of many therapeutics is inside specific cells where a drug can alter cellular biochemistry and gene regulation (Torchilin and Lukyanov 2003); however, cellular plasma membranes regulate movement of molecules into cells and present an extremely difficult barrier to these therapeutics. At intensities higher than those used in diagnostic ultrasound, ultrasonically induced cavitation has been shown to reversibly disrupt the plasma membranes of cells (Pitt et al. 2004; Ferrara et al. 2007; Postema and Gilja 2007). In this way, ultrasound has been shown to deliver small molecules, proteins and DNA into cells *in vitro*, as well as target cellular sites in *ex vivo* tissues and *in vivo* animal models (Bekeredjian et al. 2005; Hernot and Klibanov 2008). Many researchers have built upon this foundation to use ultrasound for delivery of chemotherapeutics and other drugs to cells and tissues *in vitro* and *in vivo* (Ng and Liu 2002; Dijkmans et al. 2004; Rosenthal et al. 2004).

Although ultrasound has the potential to facilitate intracellular therapies, its use has been hampered by the lack of predictability and controllability resulting from heterogeneity of ultrasound-induced bioeffects (Barnett et al., 1994; Guzman et al. 2001b; Dalecki 2004). At higher acoustic energies, where intracellular loading is the greatest, cell viability can drop dramatically (Cochran and Prausnitz 2001; Guzman et al. 2001a; Keyhani et al. 2001). Immediate loss of cell viability

Address correspondence to: Dr. M. R. Prausnitz, School of Chemical and Biomolecular Engineering, Georgia Institute of Technology, Atlanta, GA 30332-0100. E-mail: prausnitz@gatech.edu

after sonication has been attributed to cell lysis (Carstensen et al. 1993; Miller and Quddus 2001; Feril et al. 2004) and necrotic death from irreparable wounds to the plasma membrane (Schlicher et al. 2010).

Studies have shown that ultrasound can also cause cells to die as a result of apoptosis hours after sonication (Ashush et al. 2000; Vykhodtseva et al. 2001; Lagneaux et al. 2002; Honda et al. 2004; Feril et al. 2005). In contrast to necrosis, which is a form of traumatic cell death induced by acute cellular injury, apoptosis is a form of programmed cell death characterized by a series of intracellular biochemical events that occur over a timescale typically of hours (Bohm and Schild 2003). Honda et al. (2004) showed that apoptosis in sonicated cells can occur because of a large influx of extracellular Ca^{2+} ions across the permeabilized plasma membrane, which has also been seen in more recent studies (Juffermans et al. 2006; Kumon et al. 2007, 2009). Intracellular Ca^{2+} levels can vary depending on the bubble activity (Juffermans et al. 2006; Kumon et al. 2009), which may be related to cell membrane damage and the amount of time required to repair this damage. Furthermore, some sonicated cells retain high levels of Ca^{2+} long after ultrasound exposure, which indicates a complete loss of cell membrane integrity (Kumon et al. 2007, 2009).

Because the influx of Ca^{2+} also plays a crucial role in initiating plasma membrane repair (Terasaki et al. 1997), attempts to save cells from delayed Ca^{2+}-induced apoptotic death by chelating intracellular Ca^{2+} during sonication resulted in an increase in immediate necrotic cell death because of the cells' impaired ability to repair in the absence of calcium (Honda et al. 2004).

The overall aim of this study is to better understand the bioeffects caused to cells by high-intensity ultrasound exposure *in vitro*, both within minutes after sonication and hours after the initial exposure. We believe that a more thorough characterization of these effects may lead to a more rational design of ultrasound protocols as a drug delivery tool. Therefore, within this study, our first goal was to use flow cytometry to quantify the fraction of cells in each of four characteristic populations shortly after sonication and as a function of time for up to 6 h after sonication: (i) cells that appear largely unaffected; (ii) cells reversibly permeabilized, as evidenced by intracellular uptake of molecules and cell viability; (iii) cells rendered nonviable during sonication, as shown by an irreversible loss of the plasma membrane barrier or lysis of the cell into debris; and (iv) cells that appear to be viable shortly after sonication, but later undergo apoptosis and die. Applications of ultrasound often seek to maximize the second population, to achieve intracellular drug or gene delivery, and minimize the third and fourth populations, which consist of nonviable cells.

Our second goal was to test the hypothesis that highly permeabilized cells take up high levels of calcium, which are associated with subsequent induction of apoptosis (Honda et al. 2004). This hypothesis was tested using calcein and sulforhodamine as intracellular uptake markers of cell permeabilization, fluo-4 AM as a marker of intracellular calcium levels and annexin V as a marker of apoptosis.

Our third goal was to test the hypothesis that the addition of a calcium chelator immediately after sonication can save cells from apoptosis by returning cells to homeostasis through the removal of high levels of internalized calcium present because of transport through sonication-induced wounds. We chelated calcium using BAPTA-AM immediately after sonication, based on the expectation that an influx of external calcium is required at the time of sonication to help initiate cellular repair of the plasma membrane (McNeil and Steinhardt 2003), but should be chelated shortly after to prevent initiation of apoptosis.

MATERIALS AND METHODS

Cell culture

DU 145 prostate-cancer cells (American Type Culture Collection, Manassas, VA, USA) were grown to 80% confluence on T-150 flasks (BD Falcon, Franklin Lakes, NJ, USA) in growth media (RPMI-1640, Cellgro, Herndon, VA, USA) supplemented with 10% fetal bovine serum (Atlanta Biologicals, Atlanta, GA, USA) at 37 °C, 5% CO_2 and 90% relative humidity before harvest by trypsinization using previously described protocols (Keyhani et al. 2001).

Ultrasound apparatus

The ultrasound apparatus consisted of a cylindrical piezoelectric transducer (Channel Industries, Santa Barbara, CA, USA) sealed between two polyvinyl chloride pipes (5.1 cm inner diameter), as described previously (Cochran and Prausnitz 2001). This chamber was filled with deionized water that was degassed for at least 2 h in a bell jar using a vacuum pump to reduce cavitation in the water bath surrounding the cellular samples.

Ultrasound was generated at 24 kHz by a function generator (DS354 SRI, Stanford Research Systems, Sunnyvale, CA, USA). Such low-frequency ultrasound was selected because it readily generates cavitation without the need for contrast agents or other added nucleation sites. The pulsed signal was sent to an amplifier (Macro-Tech 2410, Crown Audio, Elkhart, IN, USA) that controlled the transducer *via* a matching transformer (MT-56R, Krohn-Hite, Avon, MA, USA). Using this system, the frequency, duty cycle, incident pressure and pulse length were set. The exposure time was controlled

manually. The peak ultrasound pressure was found using a calibrated hydrophone (Model TC4013, Reson, Goleta, CA, USA). Samples were exposed at room temperature to 20 acoustic pulses at a rate of 1 pulse per second. Each pulse applied 24 kHz ultrasound at a peak positive pressure of either 0.36 MPa or 0.54 MPa, with a burst length of 2400 cycles (0.1-s burst duration). Sham exposure samples (nonsonicated controls) were prepared identically to the sonicated samples, but no ultrasound was applied.

Ultrasound exposure

Following established protocols (Cochran and Prausnitz 2001), well-mixed cell suspensions at a concentration of 10^6 cells/mL in cellular growth media with fetal bovine serum were introduced into 1.2-mL sample chambers (No. 241 SEDI-PET transfer pipets, SAMCO, San Fernando, CA, USA; approximately 5.5 cm in length and 1 cm in diameter) using a 22-gauge needle and 3-mL syringe. After the chamber was filled, a stainless steel rod (1.6-mm diameter) was inserted into the pipet stem to seal the chamber and provide a means to suspend the chamber in the water bath. Sample chambers were then positioned in the exposure chamber water bath by fixing the end of the suspending rod into the chamber cover at a location that positioned the sample chamber in the axial and radial center of the transducer. Ultrasound exposure using this system has been previously shown to induce cavitation within the sample chamber. When measuring the pressure inside our exposure vessel with a hydrophone (as discussed in the manuscript), the output was a symmetric sinewave signal centered at zero. We therefore believe the peak rarefactional pressure was equal to the peak positive pressure. Furthermore, the variation in acoustic pressure within the chamber was found to be less than 10% in the radial direction and less than 20% in the axial direction (Cochran and Prausnitz 2001).

Quantification of intracellular uptake

To study uptake, cells were sonicated in cellular growth media (with serum) in the presence of either 10 μM calcein (Life Technologies, Carlsbad, CA, USA), a plasma membrane-impermeant green-fluorescent marker or 10 μM sulforhodamine 101 (Life Technologies), a plasma membrane-impermeant red-fluorescent marker. After exposure, samples were allowed to recover from the effects of sonication for 10 min at room temperature and then spun down at room temperature for 6 min at 1000x g to remove excess label from the extracellular medium. This was followed by washing at least twice in phosphate-buffered saline (PBS, Cellgro) and then assaying *via* flow cytometry, as described next. To determine the amount of intracellular calcein uptake in terms of molecules per cell, fluorescein isothiocyanate (FITC)–calibration beads were used as described previously (Guzman et al. 2001a).

Flow cytometric analysis

Samples were run on a BD-LSR flow cytometer using fluorescence-activated cell sorter DiVa software (BD Biosciences, Franklin Lakes, NJ, USA) based on previously described methods (Guzman et al. 2001a). A flow cytometer makes rapid measurements of light scatter and fluorescence on a cell-by-cell basis. In this way, statistical information on large populations of individual cells can be obtained, which provides much more detailed information about population behavior than, for example, bulk measurements made on the whole population at once. In this study, relative cellular size was obtained through measurement of the light scattering properties of the cells as detected by forward scatter (FSC) measurements. The fluorescence of green marker compounds (including calcein and fluo-4 AM) was measured with a 488-nm argon laser excitation and a 530/30 bandpass filter for emission. Red-fluorescent propidium iodide was also excited at 488 nm and measured using a 675/20 nm bandpass filter for emission. For each sample, 3×10^5 events were collected from a gated region known from previous work (Canatella et al. 2001) to contain intact DU 145 cells. Data were analyzed using FCS Express (De Novo Software, Thornhill, ON, Canada) flow cytometry analysis software.

Quantification of cell viability

To determine cellular viability, 7.5 μM propidium iodide (PI), a viability marker that fluoresces red upon binding to DNA, was added to cell samples at least 5 min before assaying via flow cytometry and at least 15 min after sonication. Cells that internalized PI were interpreted as nonviable. The fraction of nonviable cells was determined as the sum of PI-positive cells and cells lysed by sonication divided by the total cells (*i.e.*, PI-positive cells, PI-negative cells and cells lysed into debris). Although PI-positive and PI-negative cells were counted directly on the flow cytometer, quantification of cells lysed into debris was more difficult, because a single lysed cell produced multiple debris events.

The percentage of lysed cells was determined by recording the amount of time required to collect 3×10^5 cells in each sample (based on the observation that the volumetric flow rate of carrier fluid in the flow cytometer is constant). Because loss of cells caused by lysis resulted in longer collection times for sonicated samples (*i.e.*, the sonicated samples have a lower cell concentration), the number of lost cells was calculated as the balance of cells that would be required for the sonicated samples to have the same flow cytometry collection time as the control samples. Cellular populations were then quantified as either a percentage of the total cells for short-term viability

and uptake assays or as a percentage of intact cells for long-term cell death assays. Intact cells are defined as all cells that retain plasma membrane integrity 10 min after sonication.

Determination of intracellular calcium

Fluo-4 AM (Life Technologies) fluoresces green upon binding to Ca^{2+} in live cells (June and Moore 2004) and is permeant to intact plasma membranes. Thus, live intact cells with increased intracellular Ca^{2+} can be identified by measuring fluo-4 fluorescence intensity using flow cytometry. To load cells with this probe, a stock solution of fluo-4 AM was dissolved in dimethyl sulfoxide (Sigma-Aldrich, St. Louis, MO, USA) at a concentration of 5 mM, which was added to cellular samples after ultrasound exposure at the same postsonication incubation times specified for the apoptosis assay listed here later, and had a final fluo-4 AM concentration of 5 μM. Samples were then incubated in the presence of fluo-4 AM at room temperature for 30 min, washed once in PBS and assayed via flow cytometry.

Determination of apoptosis

One of the first identifiable events in the cascade of apoptosis is the translocation of phosphatidyl serine (PS) from the inner to the outer leaflet of the plasma membrane in intact cells. Fluorescently-conjugated annexin V (Life Technologies) molecules bind to exposed phosphatidyl serine, which identifies early apoptotic cells that exclude PI because of their intact plasma membranes (van Engeland et al. 1998). Necrotic cells are identified as positive for both annexin V and PI staining because of their compromised membranes.

To carry out this assay, cells were incubated for (i) 4–24 h at 37 °C or (ii) up to 2 h at room temperature after sonication. The cells were then suspended in annexin-binding buffer (prepared using the product protocol from Life Technologies) and incubated with either 5 μL FITC- or Alexa Fluor 594-conjugated annexin V stock solution (Life Technologies) per 100 μL cell suspension containing 7.5 μM PI. Each sample was analyzed *via* flow cytometry after 15 min of incubation at room temperature.

Calcium chelation

BAPTA-AM (Sigma-Aldrich) is a cell-permeant Ca^{2+} chelator in live cells (Ahluwalia et al. 2001), which means that the BAPTA-AM molecules are able to enter cells, bind and form a complex with Ca^{2+} molecules and thereby effectively sequester the Ca^{2+} from interaction with other molecules. For chelation, a stock solution containing 130 mM BAPTA-AM in dimethyl sulfoxide was added to cell suspensions 1 min after sonication at a final concentration of 130 μM. Cells were incubated with BAPTA-AM at room temperature for 30 min and then washed once in PBS. Samples were incubated at 37 °C for 6 h and then assayed according to the annexin V protocol described here before.

Statistical analysis

All means shown were calculated with at least $n = 12$ replications. The error bars shown in all figures indicate the standard error of the mean. The standard error of the mean was used because each experiment collected data from 3×10^5 events on the flow cytometer, from which mean values were calculated. Data reported in the figures provide the mean of the means from at least 12 replicate experiments. Statistical differences between treatment groups were found by Student's *t*-test or analysis of variance (ANOVA) with a 95% confidence interval ($p = 0.05$).

RESULTS

Identification and quantification of cell populations after sonication

The first goal of this study was to use flow cytometry to categorize sonicated cells into populations based on intracellular uptake and cell viability and to quantify the fraction of cells in each of these populations shortly after sonication. We identified cell populations initially by measuring forward light scatter, which measures relative cell size, and propidium iodide (PI) fluorescence, which assays cell viability determined by plasma membrane exclusion of the dye. These measurements were made 15–30 min after sonication ended, which is longer than the transient state of membrane permeability associated with ultrasound (Schlicher et al. 2006). Thus, propidium iodide labeling is interpreted as identifying nonviable cells (*i.e.*, irreversibly permeabilized).

To clarify continued discussion, we offer the following definitions. *Total cells* refers to all cells present before any treatment. *Cells* refers to events identified in the flow cytometer with forward scatter similar to that of control cells (*i.e.*, Populations 1 and 2, as defined later). *Debris* refers to events with much smaller forward scatter and is interpreted as remnants from cells lysed by sonication (*i.e.*, Population 3). *Intact cells* are cells that exclude PI, which includes viable cells and cells undergoing early-stage apoptosis.

To quantify the effects of sonication on DU 145 cells, we used flow cytometric parameters to group the cells into characteristic populations. As shown in Fig. 1a, in the absence of ultrasound, most cells exhibited strong forward scatter and weak propidium iodide fluorescence. This is consistent with a population of intact, viable cells. We have labeled this group of *intact cells* as Population 1. In Fig. 1a (nonsonicated cells), 98 ± 23% of cells fell in the category of intact cells (Population 1), as shown in Fig. 1e.

After cells were exposed to strong sonication at 0.54 MPa, many additional cellular outcomes become evident,

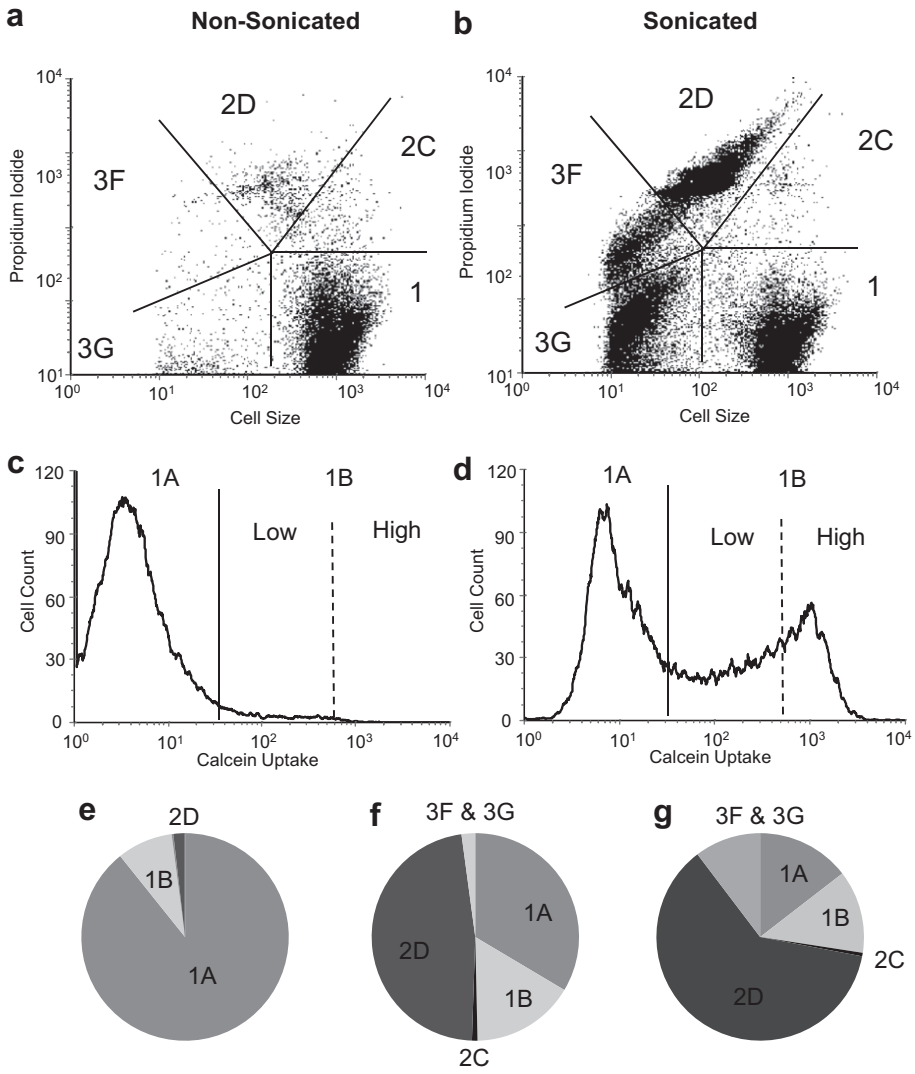

Fig. 1. Cellular populations before and after ultrasound exposure. (a) A flow cytometry plot of propidium iodide-staining *versus* cell size for nonsonicated samples shows cells mainly designated as intact cells (Population 1). (b) Within 30 min after sonication at 0.54 MPa, the distribution of total cells partially shifts into nonviable populations (Populations 2 and 3). (c) A histogram of calcein uptake among intact cells shows background fluorescence in a nonsonicated sample corresponding predominantly to no-uptake cells (Population 1A). (d) The sonicated cells show increased intracellular calcein, resulting in uptake cells (Population 1B) distributed among ''low'' and ''high'' levels of uptake. The black curve corresponds to cells assayed within 30 min after sonication at 0.54 MPa and the grey curve corresponds to the same cells assayed after 6 h. (e) A pie chart shows that nonsonicated cells are mostly no-uptake cells (Population 1A). (f) When cells are sonicated at 0.36 MPa, 50 ± 16% of total cells become nonviable cells and cellular debris (Populations 2 and 3); among intact cells, 32 ± 12% are uptake cells (Population 1B). (g) At 0.54 MPa sonication, 72 ± 18% of cells lose viability (Populations 2 and 3), and 47 ± 11% of the intact cells are uptake cells (Population 1B). Pie charts show averaged data from $n = 18$ replicates.

as shown in Fig. 1b and summarized in Fig. 1g. Figure 1f contains similar data collected after moderate sonication at 0.36 MPa. Focusing first on the population of intact cells, we see that just half of the cells (50 ± 16%) remained intact (*i.e.*, Population 1) after moderate sonication (Fig. 1f) and still fewer cells (28 ± 18%) remained intact after strong sonication (Fig. 1g).

After sonication, in addition to these intact cells there were additional populations of cells that were nonviable. A collection of nonviable cells exhibiting strong PI fluorescence is seen in the upper right quadrant of Fig. 1b. This group of *nonviable cells* is labeled as Population 2. A small minority of these cells had no change in forward scatter (1 ± 0.22% at 0.36 MPa exposure and 0.5 ± 0.21% at 0.54 MPa exposure). These cells are interpreted as *nonviable, normal-size cells* and were categorized as Population 2C. In contrast, most PI-positive cells had reduced forward scatter (45 ± 11% at 0.36 MPa and 58 ± 23% at 0.54

MPa). Based on previous analysis coupling flow cytometry with microscopy (Schlicher et al. 2010), these cells were identified as wound-derived perikarya (WD-P), which are cell bodies that have lost cytosol and consist of nuclei with little cytosol or affiliated plasma membrane. We categorized them as *nonviable, smaller-size cells* in Population 2D. We believe that both of these subpopulations on nonviable cells in Population 2 represent cells that experienced ultrasound-induced necrotic cell death.

Other cellular events identified by flow cytometry as Population 3 have very weak forward scatter and moderate or weak PI fluorescence. Guided by previous literature (Schlicher et al. 2010), we identified the cells in Population 3 as debris from cells lysed during sonication. The events with moderate PI fluorescence were interpreted as containing nuclear DNA and were termed *nuclear debris* in Population 3F. The events with weak PI fluorescence were interpreted as containing membrane debris without DNA and were termed *membrane debris* in Population 3G. Because these populations do not correspond to whole cells, it is difficult to directly determine how many lysed cells are responsible for the field of debris. Therefore, we estimated the number of destroyed cells as the balance of cells unaccounted for after sonication (see Materials and Methods). At moderate pressure (0.36 MPa), only 2.1 ± 7.4% of cells fell into this category, but at strong pressure (0.54 MPa), debris populations accounted for 10 ± 9.2% of the total cells.

This analysis has so far distinguished between intact cells (Population 1) and various types of nonviable cells (Populations 2 and 3). Among the intact cells, we next wanted to distinguish between those that were unaffected by sonication and those that had been reversibly permeabilized by exposure to ultrasound (*i.e.*, which are of primary interest for drug and gene delivery applications). We accomplished this by sonicating cells in the presence of a membrane-impermeant, green-fluorescent molecule, calcein and determining which cells took it up intracellularly. Using this technique, we identified two subpopulations among the intact cells (Population 1). One subpopulation showed no uptake of calcein, which we termed *no-uptake cells* in Population 1A. Another group of cells exhibited strong green fluorescence characteristic of calcein uptake, which we termed *uptake cells* in Population 1B. In contrast to PI, which was added to cells well after sonication and thereby labeled irreversibly permeabilized (*i.e.*, nonviable) cells, calcein was added before sonication. In this way, calcein uptake identifies cells reversibly permeabilized by ultrasound, because these cells permitted calcein entry initially and then retained calcein during post-sonication washing, which indicates initial permeability followed by subsequent return of plasma membrane integrity.

In Fig. 1c and 1d, we show the subset of cells analyzed in Fig. 1a and 1b that were intact cells (Population 1) as a function of their green fluorescence corresponding to uptake of calcein. As shown in Fig. 1c, most cells in the control sample (92 ± 20% of intact cells) show only background levels of green fluorescence, consistent with being no-uptake cells (Population 1A). The small number of cells showing moderately elevated calcein fluorescence (8 ± 14% of intact cells) is probably caused by calcein binding to the cell membrane and/or intracellular transport by endocytosis, even though we have labeled them as uptake cells (Population 1B).

In contrast, sonicated cells shown in Fig. 1d exhibit a range of calcein uptake levels, with a large group of intact cells having background fluorescence similar to controls (*i.e.*, no-uptake cells in Population 1A). Among the uptake cells, we further subdivided this population into two subgroups: those having high fluorescence, which we termed *high-uptake cells* in Population 1B+) and those having moderate fluorescence, which we termed *low-uptake cells* in Population 1B–. After moderate sonication (0.36 MPa), 20 ± 8.2% of intact cells were uptake cells, whereas 10 ± 6.1% were low-uptake cells and 10 ± 6.3% were high-uptake cells; and at 0.54 MPa, 39 ± 7.4% of intact cells were uptake cells, whereas 15 ± 5.2% were low-uptake cells and 24 ± 8.3% were high-uptake cells.

In summary, intact cells (Population 1) were found to be either no-uptake cells (Population 1A) or uptake cells (Population 1B), which could be further classified as low-uptake cells (Population1B–) or high-uptake cells (Population 1B+). Nonviable cells (Population 2) were found to be either normal size (Population 2C) or smaller size (Population 2D). Cellular debris (Population 3) was found to be either largely nuclear debris (Population 3F) or largely membrane debris (Population 3G). Table 1 summarizes this population nomenclature. Finally, the reader may notice that the letter ''E'' is missing from this naming convention. This has been done to keep the scheme consistent with our other publication, in which a Population 2E is identified (Schlicher et al. 2010) but is not relevant to the present study.

Table 1. List of Cellular Populations

Population number	Population name
Population 1	Intact cells
Population 1A	No-uptake cells
Population 1B	Uptake cells
Population1B-	Low-uptake cells
Population 1B+	High-uptake cells
Population 2	Nonviable cells
Population 2C	Nonviable, normal-size cells
Population 2D	Nonviable, smaller-size cells
Population 3	Cellular debris
Population 3F	Nuclear debris
Population 3G	Membrane debris

Some high-uptake cells later lose intracellular calcein

To supplement this analysis of cell populations created immediately after sonication, we next tracked possible shifts in populations that occurred over longer periods of time. Our greatest interest was to determine the fate of uptake cells (Population 1B), our main population of interest. Cells that initially had uptake and appeared viable after sonication (Population 1B) could later lose that uptake (*i.e.*, appear as no-uptake cells in Population 1A) or become nonviable (*i.e.*, appear as nonviable cells in Population 2 or cellular debris in Population 3) as a result, for example, ultrasound-induced apoptosis (Ashush et al. 2000; Lagneaux et al. 2002; Honda et al. 2004; Feril et al. 2005). We therefore monitored cells for 6 h after sonication, a time point previously identified as a maximum for the onset of early stages of apoptosis caused by ultrasound (Feril et al. 2004; Honda et al. 2004).

Figure 2 shows the fate of cells initially classified as intact cells (Population 1) for 6 h after sonication. The percentage of intact cells (Population 1) in control samples and cells exposed to 0.36-MPa ultrasound did not significantly change (Fig. 2, ANOVA $p > 0.05$). However, at 0.54 MPa, the percentage of no-uptake cells (Population 1A) increased by 11 ± 6.8% (Fig. 2a, ANOVA $p < 0.05$) and the percentage of uptake cells (Population 1B) decreased by 15 ± 7.1% (Fig. 2b, ANOVA $p < 0.03$). Because the overall percentage of intact cells (Population 1) did not significantly change over the 6-h period (*i.e.*, Population 1 cells did not shift to Population 2 or Population 3; data not shown), this indicates that a sizeable portion of uptake cells lost the ability to retain calcein (*i.e.*, cells shifted from uptake cells in Population 1B to no-uptake cells Population 1A) over a period of hours after sonication.

To further characterize which cells were not able to retain calcein (shift out of the uptake cells group in Population 1B), we subdivided the analysis to separately track low-uptake cells (Population 1B–) from high-uptake cells (Population 1B+). As shown in Fig. 2c, at both pressures studied, the percentage of low-uptake cells (Population 1B–) did not significantly change (ANOVA $p > 0.05$). The percentage of high-uptake cells (Population 1B+) present after exposure to 0.36-MPa

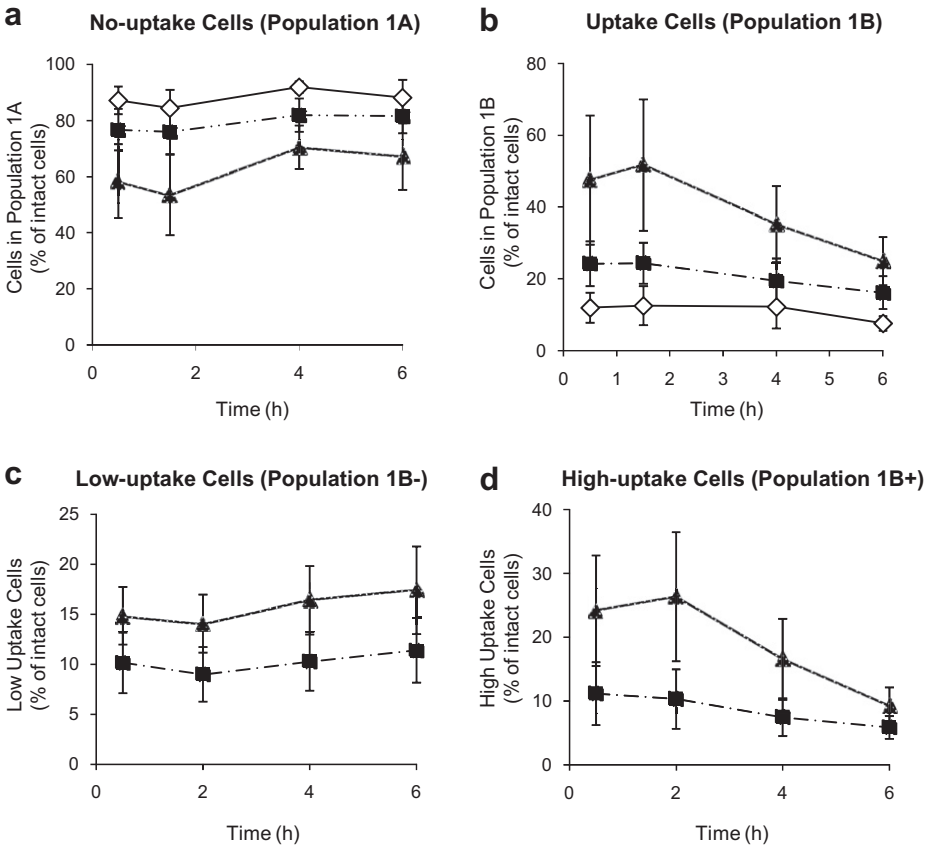

Fig. 2. Percent of intact cells among different cellular populations as a function of time at three ultrasound conditions: non-sonicated (*diamonds*) and sonicated at 0.36 MPa (*squares*) and 0.54 MPa (*triangles*). (a) No-uptake cells (Population 1A) in samples exposed to 0.54 MPa increased after 6 h postsonication. (b) Correspondingly, uptake cells (Population 1B) in samples exposed to 0.54 MPa decreased after 6 h postsonication. (c) The percentage of low-uptake cells (Population 1B–) did not change over the course of 6 h. (d) However, at 0.54 MPa, high-uptake cells (Population 1B+) decreased after 6 h. All graphs show the average ± standard error of the mean for $n = 15$ replicates.

ultrasound also did not significantly change (ANOVA $p > 0.11$). However, there was a 15 ± 6.4% decrease in high-uptake cells (Population 1B+) after exposure to 0.54-MPa ultrasound (Fig. 2d, ANOVA $p < 0.01$). Altogether, this indicates that the loss of uptake cells (Population 1B) comes largely from cells that were initially classified as high-uptake cells (Population 1B+), *i.e.*, cells that were more extensively permeabilized. These cells are known to take up high levels of calcein, but could also take up high levels of other apoptosis-inducing compounds because of their highly permeabilized state.

This led us to the hypothesis that highly permeabilized cells take up especially high levels of Ca^{2+}, which is associated with subsequent induction of apoptosis (Nicotera and Orrenius 1998). Based on previous studies that identified apoptosis in sonicated cells and the known link with elevated intracellular Ca^{2+} (Honda et al. 2004), we hypothesized that apoptosis may be responsible for the conversion of high-uptake cells (Population 1B+) into no-uptake (Population 1A). When apoptotic pathways are initiated, cellular membranes can slowly become leaky (Darzynkiewicz et al. 1992); therefore, intracellular calcein could diffuse out of the apoptotic, high-uptake cells. Although ultrasound's effects on high-uptake cells (Population 1B+) appears initially to be reversible—*e.g.*, the cells have uptake and exclude PI, indicating repair and retained viability—this additional analysis shows that some cells experience lasting effects that do not manifest themselves until hours later.

Some cells undergo apoptosis hours after sonication

To validate the hypothesis that cells can die by apoptosis hours after ultrasound exposure (Honda et al. 2004; Feril et al. 2005), we used an annexin V assay, as described in the Materials and Methods section. Figure 3a and 3b shows PI fluorescence *versus* FITC-labeled annexin V fluorescence for intact cells after sonication. As shown in Fig. 3a, nonsonicated cells have low PI and low annexin V fluorescence, consistent with viable, nonapoptotic cells (*i.e.*, intact cells in Population 1). In contrast, cells present 6 h after sonication appear among three populations: (i) low PI and low annexin V fluorescence, corresponding to viable, nonapoptotic cells (*i.e.*, intact cells Population 1, 68 ± 22% at 0.36 MPa and 58 ± 17% at 0.54 MPa); (ii) high PI and high annexin V fluorescence, corresponding to nonviable cells (*i.e.*, Population 2, 25 ± 5.1% at 0.36 MPa and 32 ± 3.2% at 0.54 MPa); and (iii) low PI and high annexin V fluorescence, corresponding to early apoptotic cells (*i.e.*, classified as intact cells in Population 1, 7.3 ± 4.0% at 0.36 MPa and 10 ± 5.1% at 0.54 MPa). These results support the hypothesis that ultrasound induces apoptosis in sonicated cells hours after the initial exposure, which can explain the observed loss of uptake cells (Population 1B) over time.

It is at first surprising that uptake cells (Population 1B) become intact, no-uptake cells (Population 1A) instead of nonviable cells (Population 2). One might expect that cells leaky enough to lose calcein should be leaky enough to be stained by PI. This apparent inconsistency may be explained by the kinetics of transport. Calcein (623 Da) and PI (668 Da) are of similar size and therefore should diffuse across a leaky cell membrane at similar rates. In our experiments, calcein leakage took place for up to 6 h, whereas PI uptake could only occur for approximately 10–15 min before flow cytometric analysis. Thus, the somewhat elevated PI levels seen among cells in the lower right quadrant of Fig. 4b may represent apoptotic cells with weakly leaky membranes (*i.e.*, small membrane disruptions that lead to a slow diffusion of calcium out of the cells over the course of hours) and the cells in the upper right quadrant are necrotic cells with highly leaky membranes (*i.e.*, large membrane disruptions that allow PI to enter the cell and stain the nuclei quickly). Whether the weakly leaky membranes are a possible cause or a result of apoptosis is unclear.

It is possible that the inability of some high-uptake cells (Population 1B+) to retain calcein (*i.e.*, become no-uptake cells in Population 1A) observed in Fig. 2 could be explained by high levels of calcein itself causing apoptosis. This is unlikely, because the data shown in Fig. 3 were generated using cells in the absence of calcein, but they nonetheless underwent apoptosis. This conclusion is also consistent with the literature, in which calcein is commonly used as an intracellular uptake marker that is considered inert (Weston and Parish 1992).

Ca^{2+} plays a major role in ultrasound-induced apoptosis

To test the hypothesis that high levels of intracellular Ca^{2+} are associated with the apoptosis observed after sonication, we labeled cells using Fluo-4 AM, a Ca^{2+}-specific fluorescent indicator, as described in the Materials and Methods section. For this analysis we excluded necrotic cells on the basis of cellular size as determined by forward scatter in the flow cytometer because, as described before (Fig. 1), more than 99% of nonviable cells had decreased forward scatter. Figure 3c shows that nonsonicated control cells exhibit low levels of intracellular Ca^{2+} and annexin V staining, consistent with normal cellular behavior. In Fig. 3d, a subpopulation of cells appears with high levels of intracellular Ca^{2+} and annexin V staining (3.4 ± 1.8% at 0.36 MPa and 8.2 ± 4.8% at 0.54 MPa), which shows that annexin-positive (*i.e.*, apoptotic) cells also show an increase in intracellular Ca^{2+}. This supports the hypothesis that

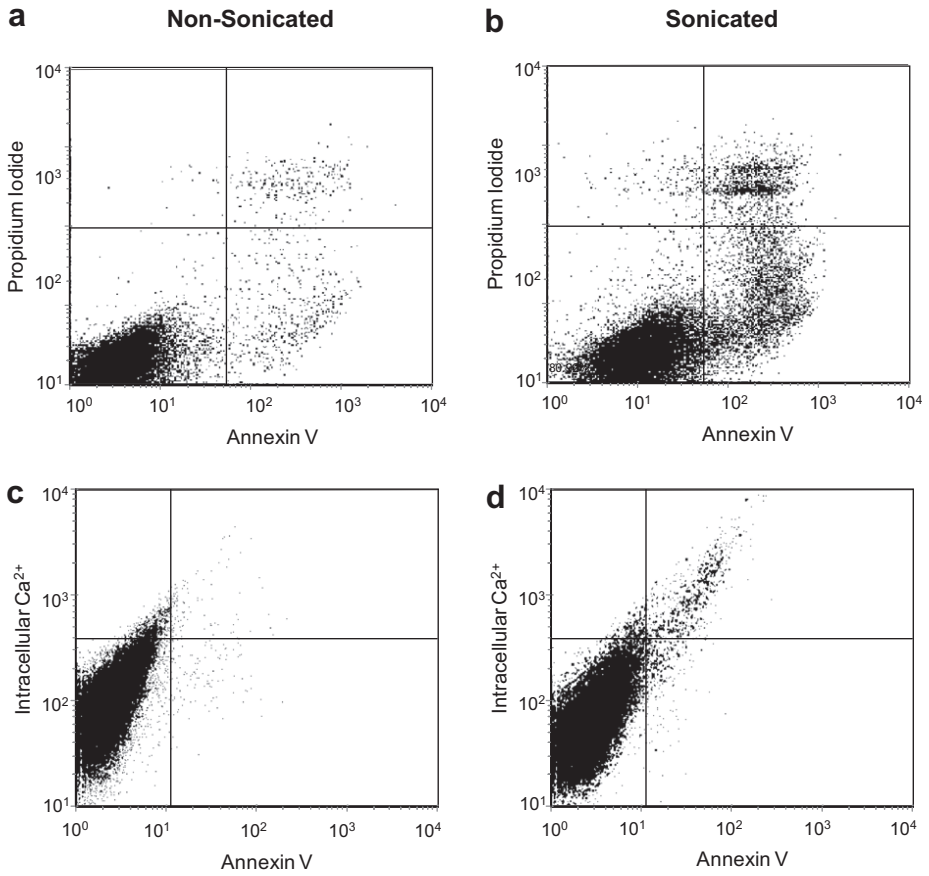

Fig. 3. Identification of apoptotic cells and their correlation with increased intracellular Ca^{2+}. Plotting propidium iodide *versus* annexin V fluorescence identifies apoptotic cells. (a) Most nonsonicated cells appear in the lower-left quadrant, indicating that they are viable (PI-negative) and not undergoing apoptosis (annexin-negative). (b) At 6 h after ultrasound exposure at 0.54 MPa, a sizeable number of cells are grouped in the lower-right quadrant, indicating that these cells are in the early stages of apoptosis (annexin-positive and PI-negative). Plotting intracellular Ca^{2+} *versus* annexin V fluorescence identifies correlation between apoptosis and intracellular Ca^{2+} levels. (c) Nonsonicated cells have background levels of intracellular Ca^{2+} and are not undergoing apoptosis. (d) In contrast, annexin V–stained apoptotic cells in sonicated (0.54 MPa) samples generally have higher levels of intracellular Ca^{2+} (upper-right quadrant). All data were taken 6 h after sonication and include all cells (*i.e.*, Populations 1 and 2) present at that time. Many necrotic (PI-positive) cells were lost during cell washing and are therefore not represented in these graphs but were accounted for in calculations presented in the text.

ultrasound-induced apoptosis is associated with, and possibly initiated by, an increase in cytosolic Ca^{2+}.

Because it appears that delayed cell death is associated with cells having high calcein uptake (Population 1B+), we next assessed the relationship between high intracellular Ca^{2+} and levels of uptake. For these studies, we used sulforhodamine 101 as our uptake marker. This molecule is similar in size to calcein, but exhibits a red fluorescence that can be used with the green fluorescent Ca^{2+} marker. Nonsonicated cells (Fig. 4a) had low levels of intracellular Ca^{2+} and sulforhodamine, as expected. In contrast, sonicated cells (Fig. 4b) contained a subpopulation with high levels of both intracellular Ca^{2+} and sulforhodamine ($7 \pm 3.2\%$ at 0.36 MPa and $12 \pm 4.6\%$ at 0.54 MPa), and essentially all cells with elevated intracellular Ca^{2+} ($> 99\%$) also exhibited sulforhodamine uptake. This observation supports the idea that the large increase in intracellular Ca^{2+} is a result of the same plasma membrane wounds that lead to sulforhodamine uptake. Moreover, the percentages of cells with high Ca^{2+} and sulforhodamine uptake (Fig 4d) closely mirror the number of cells found to be apoptotic from annexin staining (Fig. 3b, 3d), suggesting they are all the same population of cells. Although simultaneous assay of PI, annexin, uptake and Ca^{2+} would provide a more definitive correlation, technical limitations prevented us from using all of these stains at the same time in the flow cytometer.

In summary, the data show that (i) high-uptake cells have high levels of intracellular Ca^{2+}, (ii) cells with high levels of intracellular Ca^{2+} are apoptotic, (iii) apoptotic cells become evident hours after sonication and (iv) some high-uptake cells disappear (*i.e.*, lose their calcein) hours after sonication. Taken together, these observations suggest that wounds causing high uptake of calcein lead to high

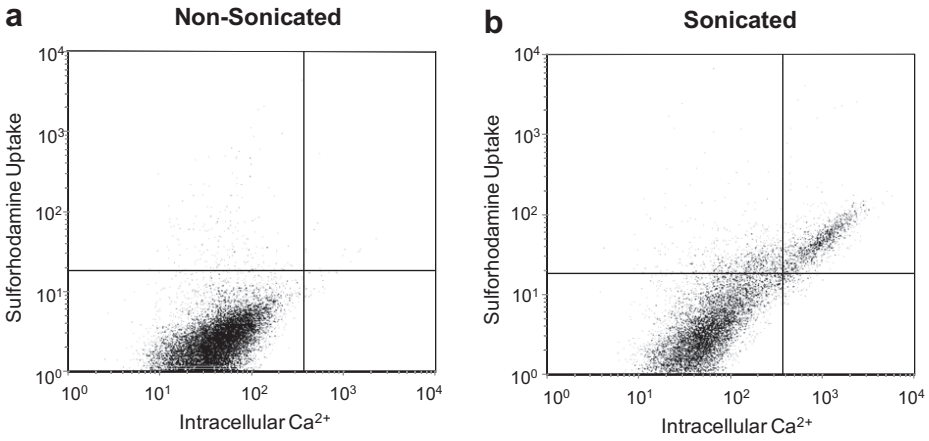

Fig. 4. Intracellular Ca^{2+} as a function of sulforhodamine uptake among intact cells assayed within 30 min after sonication. (a) Nonsonicated samples have background levels of intracellular Ca^{2+} and sulforhodamine fluorescence. (b) Cells sonicated at 0.54 MPa show a strong correlation between the levels of intracellular Ca^{2+} and sulforhodamine uptake.

levels of intracellular Ca^{2+} that contribute to inducing apoptosis.

Calcium chelation after sonication inhibits ultrasound-induced apoptosis

Given this relationship between high levels of Ca^{2+} uptake and apoptosis, we hypothesized that addition of a Ca^{2+} chelator immediately after sonication can save cells from apoptotic death. This hypothesis is based on the expectation that the chelator must not be added before sonication, because elevated intracellular Ca^{2+} is needed to initiate cellular processes to repair the plasma membrane after ultrasound-induced disruption (McNeil and Kirchhausen 2005) and thereby to allow uptake and retention to occur (Schlicher et al. 2006), but it must be added shortly after sonication to block initiation of apoptosis. If successful, this approach to saving cells from apoptosis could be valuable to applications that seek to deliver molecules into cells without killing them, such as the delivery of DNA, siRNA or other gene-based therapies into living cells to modify their protein expression patterns (Russ and Wagner 2007).

First, we validated that addition of a Ca^{2+} chelator, BAPTA AM, indeed reduced intracellular Ca^{2+} levels. As shown in the representative histogram in Fig. 5a, intracellular Ca^{2+} was significantly reduced. Of greatest interest, Ca^{2+} chelation also reduced the incidence of apoptosis. Figure 5b shows that although Ca^{2+} chelation had no effect on nonsonicated cells (Student's *t*-test, $p > 0.05$), the number of apoptotic cells was reduced among sonicated cells by 32% at 0.36 MPa (Student's *t*-test, $p = 0.01$) and by 44% at 0.54 MPa (Student's *t*-test, $p = 0.02$). Thus, Ca^{2+} chelation can save cells from apoptosis.

Additional measurements showed that Ca^{2+} chelation did not affect the percentage of calcein uptake cells (Population 1B, Fig. 5c, Student's *t*-test, $p > 0.05$) or the percentage of nonviable (necrotic) cells (Population 2, Fig. 5d, Student's *t*-test, $p > 0.05$). This indicates that Ca^{2+} chelation under these conditions inhibited apoptosis without significantly affecting other cellular processes associated with uptake and necrotic cell death, which mostly occurred before the Ca^{2+} chelator was added.

DISCUSSION

Measurement and control of cell populations created by sonication

We have shown that there are three primary cellular outcomes immediately after sonication (Fig. 6): (i) cells that appear largely unaffected by ultrasound (*i.e.*, no-uptake cells in Population 1A); (ii) cells opened temporarily to allow for intracellular uptake and then subsequently resealed (*i.e.*, uptake cells in Population 1B); and (iii) cells rendered nonviable by ultrasound, as shown by an irreversible loss of the plasma membrane barrier or lysis of the cell into debris (nonviable cells and cellular debris in Populations 2 and 3). For drug delivery and other applications, it is desirable to maximize the number of uptake cells (Population 1B) and minimize the number of nonviable cells and cellular debris (Populations 2 and 3).

These observations are consistent with previous literature, which has identified that the mechanism of sonication-induced cellular effects involves acoustically generated cavitation activity that ''wounds'' the cell's plasma membrane, thereby allowing uptake of molecules into the cells (Ellwart et al. 1988; Guzman et al. 2003; Kamaev et al. 2004; Bekeredjian et al. 2005; Zarnitsyn et al. 2008). Either these wounds are resealed by active cellular processes, allowing the cells to remain viable or they are unable to be resealed quickly enough to save the cell, which results in cell death (Schlicher et al. 2006).

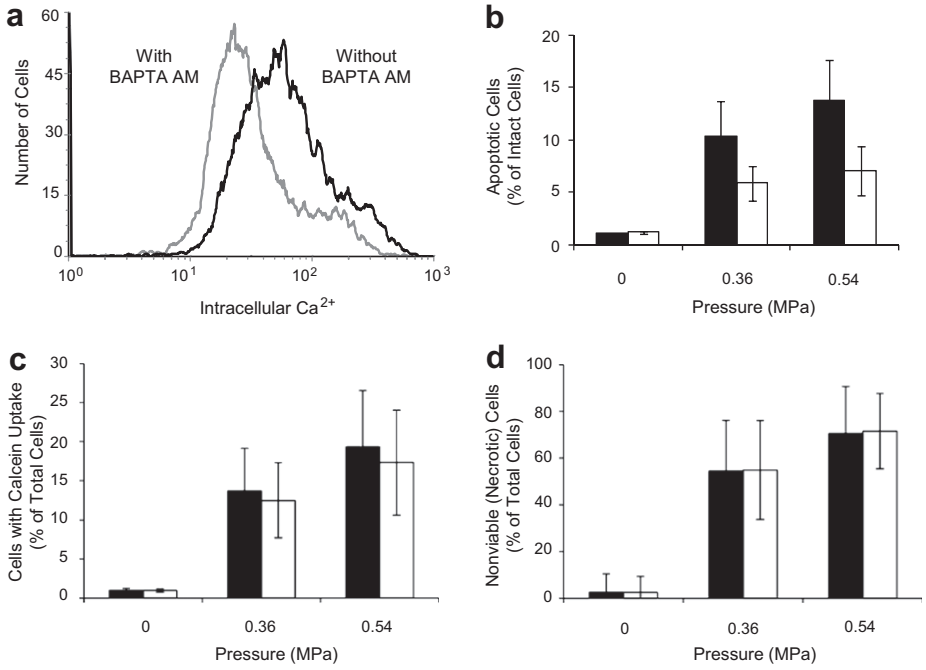

Fig. 5. The effects of Ca^{2+} chelation on cell populations after sonication at 0.54 MPa: nonchelated samples (*black line* and *black bars*) and samples chelated with BAPTA AM (*gray line* and *white bars*). (a) Ca^{2+} chelation reduced intracellular Ca^{2+} levels in intact cells. (b) Apoptosis of intact cells is decreased by 32–44% after intracellular Ca^{2+} chelation 1 min after sonication. (c) The percentage of uptake cells (Population 1B), (d) nonviable (necrotic) cells and cellular debris (Populations 2 and 3) among total cells remains unchanged after postsonication Ca^{2+} chelation. The graphs show the average ± standard error of the mean for $n = 12$ replicates.

By monitoring these populations after 6 h, we noticed that the subset of high-uptake cells (Population 1B+) was lost over time. This allowed us to identify a fourth cellular outcome that only became evident hours after sonication: (iv) cells that appear to be viable shortly after sonication, but later undergo apoptosis and die.

Because the usual goal of drug delivery applications is to load living cells with high levels of uptake, it was of concern that these high-uptake cells were subsequently losing the molecules they internalized and, as we later determined, were undergoing apoptosis. Therefore, we wanted to understand why these cells became apoptotic to intervene. Insight from previous studies (Honda et al. 2004) led us to monitor levels of intracellular Ca^{2+} as a possible mediator of apoptosis. In this way, we found that intracellular Ca^{2+} levels correlated with intracellular levels of our model drug, calcein, or sulfarhodamine. This suggested that the desired effect of drug uptake was directly tied to the undesired effect of Ca^{2+} uptake that led to apoptosis.

Consistent with previous studies (Guzman et al. 2001b; Keyhani et al. 2001), sonication at higher pressure led to higher (initial) levels of uptake; ultrasound at 0.54 MPa led to more high-uptake cells (Population 1B+; 24 ± 8.3% of intact cells) than ultrasound at 0.36 MPa (10 ± 6.3% of intact cells). However, after 6 h, samples exposed to ultrasound at 0.54 MPa had only 9.2 ± 2.9% high-uptake cells (Population 1B+), whereas samples exposed at 0.36 MPa still had 5.9 ± 1.8%. This shows that gains from increasing ultrasound pressure (and possibly other parameters, such as exposure time and energy) to increase uptake can be at least partially offset by the associated increase in apoptosis.

The sensitivity of Ca^{2+}-mediated biochemical signaling is dependent on both the concentration of the Ca^{2+} and the amount of time an increased level of Ca^{2+} exists in the cell (Berridge et al. 1998). Previous studies attempted to prevent apoptosis by chelating intracellular Ca^{2+} with BAPTA AM before sonication (Honda et al. 2004). Although this prevented apoptosis, it increased cell death by necrosis (Population 2-type death) and blocked uptake from occurring by causing wounds to be nonrepairable. We believe this is because Ca^{2+} has been shown to be an important signaling molecule in cellular wound repair, both after sonication (Schlicher et al. 2006) and other cell wounding mechanisms (Terasaki et al. 1997; McNeil and Kirchhausen 2005). In the absence of Ca^{2+}, cells cannot recruit lipid repair vesicles to the sites of plasma membrane disruption. Consequently, chelating Ca^{2+} in cells before or during sonication inhibits the ability of cells to recover normal membrane integrity after ultrasound exposure, and thus renders the cell nonviable.

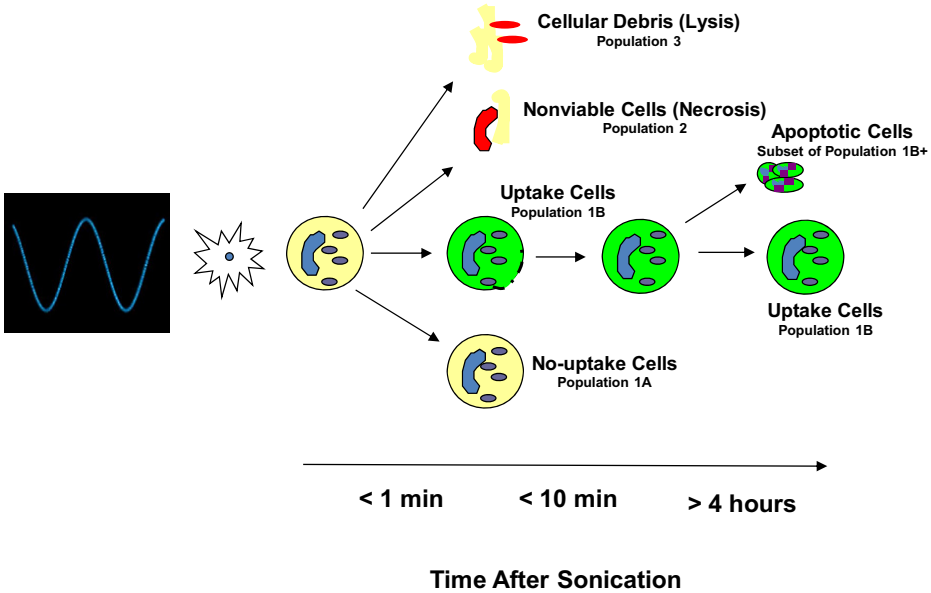

Fig. 6. Summary of cell populations and outcomes as a function of time. At the conditions used for this study, ultrasound caused extracellular cavitation—believed to be the driving force behind the observed bioeffects. Within minutes after sonication, there appear to be four types of cells: (i) cells that appear largely unaffected (*i.e.*, no-uptake cells in Population 1A); (ii) cells reversibly permeabilized (*i.e.*, uptake cells in Population 1B); (iii) necrotic cells rendered nonviable during sonication (*i.e.*, nonviable cells in Population 2); and (iv) cells lysed into debris (*i.e.*, cellular debris in Population 3). Over the course of <6 hours, a portion of the high-uptake cells (Population 1B+) can die by apoptosis, a type of programmed cell death, but other uptake cells (Population 1B) survive.

Other studies have indicated that Ca^{2+}-mediated initiation of cellular wound repair occurs on a time scale of seconds, whereas, commencement of apoptosis may take minutes (Berridge et al. 1998). Altogether, this presents a window of opportunity to save cells from apoptosis without inhibiting membrane repair mechanisms that prevent necrosis by chelating Ca^{2+} shortly after sonication (Fig. 5b). By chelating Ca^{2+} with BAPTA AM at 1 min postsonication, wound-repair pathways should be able to proceed, but apoptotic signaling pathways were alleviated. This allowed us to reduce the number of apoptotic cells without forcing cells into uncontrolled, necrotic death.

This approach to ''saving'' cells may be of direct use to laboratory applications, such as ultrasound-mediated transfection and intracellular delivery of RNAi, proteins and other compounds. *In vivo*, postsonication chelation of Ca^{2+} may be more difficult; therefore, cells might be saved by constraining exposure to ultrasound conditions that limit the extent of plasma membrane wounding to minimize the initial influx of Ca^{2+} into the cells.

Estimate of cellular wound sizes associated with apoptosis

Guided by previous literature (Guzman et al. 2001a; Zarnitsyn et al. 2008), we can estimate the size of membrane wounds associated with apoptosis. Our data show that 10% of intact cells underwent apoptosis 6 h after 0.54-MPa sonication and that these cells appear to be those with the highest levels of calcein update. To characterize these cells, we can determine the minimum calcein fluorescence associated with the 10% most fluorescent cells by examining our fluorescent histograms from the flow cytometer.

In a previous study, Guzman et al. (2001a) showed that fluorescent beads can be used to generate a calibration curve to convert arbitrary fluorescence values from the flow cytometer into absolute measures of the number of calcein molecules in each cell using the same cell type used in this study. In this way, we found that the 10% most fluorescent cells in our study had intracellular calcein levels of at least 3×10^6 molecules per cell. We therefore propose that cells that underwent apoptosis generally sustained wounds large enough to permit entry of more than 3×10^6 molecules per cell.

In another study, Zarnitsyn et al. (2008) presented a theoretical model that determined membrane wound sizes as a function of calcein uptake in the same cell type and similar ultrasound conditions as used in this study, and found that uptake increased with wound size. Equation (13) in this model predicts that calcein uptake under the conditions of our study at a level of 3×10^6 molecules per cell corresponds to a plasma membrane wound radius of approximately 100 nm. Altogether, this suggests that wounds of at least 100 nm radius are large and long-lived enough to permit entry of at least 3×10^6 calcein molecules per cell, which similarly permit

entry of intracellular Ca^{2+} at levels associated with apoptosis. We therefore hypothesize that wounds smaller than approximately 100 nm are well tolerated by cells, whereas larger wounds lead to apoptosis. This hypothesis requires further testing.

CONCLUSION

This study showed that sonication produces a heterogeneous population of cells that can: appear largely unaffected (*i.e.*, no-uptake cells in Population 1A); internalize molecules and remain viable because of reversible membrane permeabilization (*i.e.*, uptake cells in Population 1B); be rendered nonviable during sonication by an irreversible loss of the plasma membrane barrier (*i.e.*, nonviable cells in Population 2) or lysis of the cell into debris (*i.e.*, cellular debris in Population 3); or appear to be viable shortly after sonication, but later undergo apoptosis and die (some high-uptake cells in Population 1B+). Increasing pressure decreased intact cells (Population 1) and increased nonviable cells and cellular debris (Populations 2 and 3).

Further analysis indicated that the increased membrane permeabilization associated with high levels of calcein uptake were also associated with Ca^{2+} uptake, which in turn led to increased apoptosis. This suggests that there may be an upper limit to the amount of membrane wounding that a cell can tolerate before too much Ca^{2+} enters, which was estimated in this study to be approximately 100 nm in radius. Although most medical applications seek to maximize drug delivery into cells, this study suggests that moderate levels of intracellular delivery may be more desirable than high levels, because high levels of uptake lead to apoptosis. To address this limitation, we found that cells with high levels of uptake can be saved from apoptosis through the addition of a Ca^{2+} chelator. We were able to save up to 44% of apoptotic cells, and further optimization may be able to increase this number.

Overall, these conclusions suggest that ultrasound-induced viability losses are predominantly a function of the initial wound to the cellular membranes, where small wounds lead to uptake with retained viability, larger wounds lead to apoptotic death (which can be at least partially blocked by Ca^{2+} chelation) and still larger wounds cause immediate necrosis. Therefore, the key to controlling ultrasound-induced bioeffects may lie in controlling the size of these wounds and the manner by which the cells repair them.

Acknowledgments—The authors thank P.H. Yun for laboratory assistance, J. Crowe for flow cytometric assistance and discussions and V.G. Zarnitsyn for wound size calculations. This work was supported in part by the National Institutes of Health and the U.S. Department of Education GAANN program. This work was carried out at the Center for Drug Design, Development and Delivery and the Institute for Bioengineering and Bioscience at Georgia Tech. J. D. H. carried out and helped design and analyze all experiments; R. K. S. helped with experimental design and data interpretation; H. K. H. helped design and carry out the flow cytometric analyses; and M. R. P. helped design and interpret the studies and served as the principal investigator.

REFERENCES

Ahluwalia JP, Topp JD, Weirather K, Zimmerman M, Stamnes M. A role for calcium in stabilizing transport vesicle coats. J Biol Chem 2001; 276:34148–34155.

Allen TM, Cullis PR. Drug delivery systems: Entering the mainstream. Science 2004;303:1818–1822.

Ashush H, Rozenszajn LA, Blass M, Barda-Saad M, Azimov D, Radnay J, Zipori D, Rosenschein U. Apoptosis induction of human myeloid leukemic cells by ultrasound exposure. Cancer Res 2000; 60:1014–1020.

Barnett SB, ter Haar GR, Ziskin MC, Nyborg WL, Maeda K, Bang J. Current status of research on biophysical effects of ultrasound. Ultrasound Med Biol 1994;20:205–218.

Bekeredjian R, Grayburn PA, Shohet RV. Use of ultrasound contrast agents for gene or drug delivery in cardiovascular medicine. J Am Coll Cardiol 2005;45:329–335.

Berridge MJ, Bootman MD, Lipp P. Calcium—a life and death signal. Nature 1998;395:645–648.

Bohm I, Schild H. Apoptosis: the complex scenario for a silent cell death. Mol Imaging Biol 2003;5:2–14.

Canatella PJ, Karr JF, Petros JA, Prausnitz MR. Quantitative study of electroporation-mediated molecular uptake and cell viability. Biophys J 2001;80:755–764.

Carstensen EL, Kelly P, Church CC, Brayman AA, Child SZ, Raeman CH, Schery L. Lysis of erythrocytes by exposure to CW ultrasound. Ultrasound Med Biol 1993;19:147–165.

Cochran SA, Prausnitz MR. Sonoluminescence as an indicator of cell membrane disruption by acoustic cavitation. Ultrasound Med Biol 2001;27:841–850.

Dalecki D. Mechanical bioeffects of ultrasound. Annu Rev Biomed Eng 2004;6:229–248.

Darzynkiewicz Z, Bruno S, Del Bino G, Gorczyca W, Hotz MA, Lassota P, Traganos F. Features of apoptotic cells measured by flow cytometry. Cytometry 1992;13:795–808.

Dijkmans PA, Juffermans LJ, Musters RJ, van Wamel A, ten Cate FJ, van Gilst W, Visser CA, de Jong N, Kamp O. Microbubbles and ultrasound: from diagnosis to therapy. Eur J Echocardiogr 2004;5:245–256.

Ellwart JW, Brettel H, Kober LO. Cell membrane damage by ultrasound at different cell concentrations. Ultrasound Med Biol 1988;14:43–50.

Feril J, Loreto B, Kondo T, Takaya K, Riesz P. Enhanced ultrasound-induced apoptosis and cell lysis by a hypotonic medium. Int J Radiat Biol 2004;80:165–175.

Feril LB Jr, Kondo T, Cui ZG, Tabuchi Y, Zhao QL, Ando H, Misaki T, Yoshikawa H, Umemura S. Apoptosis induced by the sonomechanical effects of low intensity pulsed ultrasound in a human leukemia cell line. Cancer Lett 2005;221:145–152.

Ferrara K, Pollard R, Borden M. Ultrasound microbubble contrast agents: Fundamentals and application to gene and drug delivery. Annu Rev Biomed Eng 2007;9:415–447.

Guzman HR, McNamara AJ, Nguyen DX, Prausnitz MR. Bioeffects caused by changes in acoustic cavitation bubble density and cell concentration: A unified explanation based on cell-to-bubble ratio and blast radius. Ultrasound Med Biol 2003;29:1211–1222.

Guzman HR, Nguyen DX, Khan S, Prausnitz MR. Ultrasound-mediated disruption of cell membranes. I. Quantification of molecular uptake and cell viability. J Acoust Soc Am 2001a;110:588–596.

Guzman HR, Nguyen DX, Khan S, Prausnitz MR. Ultrasound-mediated disruption of cell membranes. II. Heterogeneous effects on cells. J Acoust Soc Am 2001b;110:597–606.

Hernot S, Klibanov AL. Microbubbles in ultrasound-triggered drug and gene delivery. Adv Drug Deliv Rev 2008;60:1153–1166.

Honda H, Kondo T, Zhao Q-L, Feril J, Loreto B, Kitagawa H. Role of intracellular calcium ions and reactive oxygen species in apoptosis induced by ultrasound. Ultrasound Med Biol 2004;30:683–692.

Juffermans LJ, Dijkmans PA, Musters RJ, Visser CA, Kamp O. Transient permeabilization of cell membranes by ultrasound-exposed

microbubbles is related to formation of hydrogen peroxide. Am J Physiol Heart Circ Physiol 2006;291:H1595–H1601.
June CH, Moore JS. Measurement of intracellular ions by flow cytometry. Curr Protoc Immunol 2004. Chapter 5:Unit 5.
Kamaev PP, Hutcheson JD, Wilson ML, Prausnitz MR. Quantification of optison bubble size and lifetime during sonication dominant role of secondary cavitation bubbles causing acoustic bioeffects. J Acoust Soc Am 2004;115:1818–1825.
Keyhani K, Guzman HR, Parsons A, Lewis TN, Prausnitz MR. Intracellular drug delivery using low-frequency ultrasound: Quantification of molecular uptake and cell viability. Pharm Res 2001;18:1514–1520.
Kumon RE, Aehle M, Sabens D, Parikh P, Han YW, Kourennyi D, Deng CX. Spatiotemporal effects of sonoporation measured by real-time calcium imaging. Ultrasound Med Biol 2009;35:494–506.
Kumon RE, Aehle M, Sabens D, Parikh P, Kourennyi D, Deng CX. Ultrasound-induced calcium oscillations and waves in Chinese hamster ovary cells in the presence of microbubbles. Biophys J 2007;93:L29–L31.
Lagneaux L, de Meulenaer EC, Delforge A, Dejeneffe M, Massy M, Moerman C, Hannecart B, Canivet Y, Lepeltier MF, Bron D. Ultrasonic low-energy treatment: A novel approach to induce apoptosis in human leukemic cells. Exp Hematol 2002;30:1293–1301.
Langer R. Drug delivery. Drugs on target. Science 2001;293:58–59.
McNeil PL, Kirchhausen T. An emergency response team for membrane repair. Nat Rev Mol Cell Biol 2005;6:499–505.
McNeil PL, Steinhardt RA. Plasma membrane disruption: repair, prevention, adaptation. Annu Rev Cell Dev Biol 2003;19:697–731.
Miller DL, Quddus J. Lysis and sonoporation of epidermoid and phagocytic monolayer cells by diagnostic ultrasound activation of contrast agent gas bodies. Ultrasound Med Biol 2001;27:1107–1113.
Ng KY, Liu Y. Therapeutic ultrasound: Its application in drug delivery. Med Res Rev 2002;22:204–223.
Nicotera P, Orrenius S. The role of calcium in apoptosis. Cell Calcium 1998;23:173–180.
Pitt WG, Husseini GA, Staples BJ. Ultrasonic drug delivery—a general review. Expert Opin Drug Deliv 2004;1:37–56.
Postema M, Gilja OH. Ultrasound-directed drug delivery. Curr Pharm Biotechnol 2007;8:355–361.
Rosenthal I, Sostaric JZ, Riesz P. Sonodynamic therapy—a review of the synergistic effects of drugs and ultrasound. Ultrason Sonochem 2004;11:349–363.
Russ V, Wagner E. Cell and tissue targeting of nucleic acids for cancer gene therapy. Pharm Res 2007;24:1047–1057.
Schlicher RK, Hutcheson JD, Apkarian RP, Prausnitz MR. Changes in cell morphology due to plasma membrane wounding by acoustic cavitation. Ultrasound Med Biol 2010;36:677–692.
Schlicher RK, Radhakrishna H, Tolentino TP, Apkarian RP, Zarnitsyn V, Prausnitz MR. Mechanism of intracellular delivery by acoustic cavitation. Ultrasound Med Biol 2006;32:915–924.
Terasaki M, Miyake K, McNeil PL. Large plasma membrane disruptions are rapidly resealed by Ca2+-dependent vesicle-vesicle fusion events. J Cell Biol 1997;139:63–74.
Torchilin VP, Lukyanov AN. Peptide and protein drug delivery to and into tumors: Challenges and solutions. Drug Discov Today 2003;8:259–266.
van Engeland M, Nieland LJ, Ramaekers FC, Schutte B, Reutelingsperger CP. Annexin V-affinity assay: A review on an apoptosis detection system based on phosphatidylserine exposure. Cytometry 1998;31:1–9.
Vykhodtseva N, McDannold N, Martin H, Bronson RT, Hynynen K. Apoptosis in ultrasound-produced threshold lesions in the rabbit brain. Ultrasound Med Biol 2001;27:111–117.
Weston SA, Parish CR. Calcein: A novel marker for lymphocytes which enter lymph nodes. Cytometry 1992;13:739–749.
Zarnitsyn V, Rostad CA, Prausnitz MR. Modeling transmembrane transport through cell membrane wounds created by acoustic cavitation. Biophys J 2008;95:4124–4138.